Transient current induced in thin film diamonds by swift heavy ions

Shin-Ichiro Sato, Takahiro Makino, Takeshi Ohshima, Tomihiro Kamiya, Wataru Kada, Osamu Hanaizumi, Veljko Grilj, Natko Skukan, Michal Pomorski, Gyorgy Vizkelethy

Title:

Transient Current Induced in Thin Film Diamonds by Swift Heavy Ions

Authors:

Shin-ichiro Sato[a,*], Takahiro Makino[a], Takeshi Ohshima[a], Tomihiro Kamiya[a], Wataru Kada[b], Osamu Hanaizumi[b], Veljko Grilj[c], Natko Skukan[c], Ivan Sudić[c], Milko Jakšić[c], Michal Pomorski[d], Gyorgy Vizkelethy[e*]

Affiliation:

[a]Quantum Beam Science Research Directorate (QuBS), National Institutes for Quantum and Radiological Science and Technology (QST), Takasaki, Gunma 370-1292, 370-1292

[b]Division of Electronics and Informatics, Faculty of Science and Technology, Gunma University, Kiryu, Gunma 376-8515, Japan

[c]Division for Experimental Physics, Ruđer Bošković Institute (RBI), 10000 Zagreb, Croatia

[d]CEA-LIST, Diamond Sensors Laboratory, Gif-sur-Yvette F-091191, France

[e]Sandia National Laboratories (SNL), P.O. Box 5800, Albuquerque, NM 87185-1056, USA

Corresponding Author: Shin-ichiro Sato (S-I. Sato)

Tel: +81-27-346-9378; E-mail: sato.shinichiro2@qst.go.jp

* *Sandia National Laboratories is a multi-program laboratory managed and operated by Sandia Corporation, a wholly owned subsidiary of Lockheed Martin Corporation, for the U.S. Department of Energy's National Nuclear Security Administration under contract DE-AC04-94AL85000.*

Key Words:

Diamond crystal, radiation induced effects, detectors, membranes

Abstract

Single crystal diamond is a suitable material for the next generation particle detectors because of the superior electrical properties and the high radiation tolerance. In order to clarify fundamental characteristics of diamond particle detectors, transient currents generated in diamonds by single swift heavy ions (26 MeV O^{5+} and 45 MeV Si^{7+}) were investigated. Two dimensional mappings of transient currents by single ion hits were also measured. In the case of 50 μm-thick diamond, both the signal height and the collected charge were reduced by the subsequent of ion hits and the charge collection time was extended. Strong signals appeared occasionally when most of the signals were fully degraded. These results were thought to be attributable to the polarization effect in diamond and it appeared only at the positive bias. In the case of 6 μm-thick diamond membrane, an "island" structure was found in the 2D mapping of transient currents. Signals in the islands showed different applied bias dependence from signals in other regions, indicating different crystal quality. The instability of signals resulting from the polarization effect was also observed in the 6 μm-thick diamond membrane. Simulation study of transient currents based on the Shockley-Ramo theorem clarifies that the polarization appears only in the irradiated region and both the electric field and the hole lifetime are reduced by the polarization effect.

1. Introduction

Diamond is an attractive material for radiation detectors to be used in harsh environments because of its superior electronic properties, such as high carrier mobility, wide bandgap, high radiation tolerance, and high breakdown voltage. Although the study for diamond radiation detectors started in the 1940s [1, 2], many problems about the sample preparation, such as availability, crystal quality, and control of impurity, made the development difficult because natural diamonds were used in the earliest years. Since significant improvement has been recently achieved in the crystal growth technology of diamond, research and development for single-crystal diamond radiation detectors has been extensively carried out in recent years and their superior characteristics has been demonstrated [3]. For instance, it has been recently reported that single-crystal diamonds grown by chemical vapor deposition (CVD) showed almost 100 % charge collection efficiency and high energy resolution (less than 1 %) in the detection of 5.486 MeV alpha particles from ^{241}Am [4].

With the development of research on diamond particle detectors, however, some issues has also come out. One of the critical issues on diamond particle detectors is the polarization effect: temporal degradation of signal amplitude during ion irradiation. Being generally known to occur in insulator crystals [5], the polarization effect has been one of the important topics of interest in diamond detectors [6-8]. The polarization effect

disappears by changing the polarity of applied bias and occasionally mitigated during ion irradiation [9]. This is more pronounced for short range ions, which produce high ionization in a small volume [10]. When charge carriers generated by radiation are trapped in deep levels in diamond, they cannot be released in a short time and give rise to a space charge (internal electric field). The external electric field is screened by the space charge and as a result, the collected charge signal amplitude decreases. This is a brief explanation of the polarization effect, and the detail mechanism is still less well understood. The origin of these deep levels is completely unidentified. It is also still unclear how the charge collection process of generated carriers are affected by the polarization effect.

In this study, transient currents in diamond generated by swift heavy ions were measured using Time Resolved Ion-Beam Induced Current (TRIBIC) technique [11] in order to investigate the charge collection process in diamonds. The TRIBIC technique is a powerful tool for investigating the collection process of generated charge by incident ions. Two dimensional distribution of transient currents was also investigated.

2. Experimental

Two samples were used in this study: a single-crystal CVD (sc-CVD) diamond with the thickness of 50 μm and a thin sc-CVD diamond membrane with the thickness of 6 μm. The fabrication method of diamond membrane was reported elsewhere [12]. The detectors were of electrical grade (substitutional nitrogen content [N] < 5 ppb) and optical grade ([N] < 5 ppm), respectively, which were commercially available from Element Six Ltd. Metal electrodes were formed on both sides of the samples to collect charges

generated by incident ions (26 MeV O^{5+} and 45 MeV Si^{7+}). Current-voltage (IV) and capacitance-voltage (CV) characteristics were investigated prior to TRIBIC measurements.

The experimental setup of TRIBIC measurement is illustrated in Fig. 1. Comparing to conventional Ion Beam Induced Charge (IBIC) technique [13], the TRIBIC measurement gives information on time variation of charge collection, i.e. transient current, in addition to generated charge by a single ion incidence. The detail of TRIBIC measurement system was reported elsewhere [11]. The samples were irradiated at normal incidence with a focused microbeam of 26 MeV O^{5+} and 45 MeV Si^{7+} ions at the Sandia National Laboratories (SNL), USA. Ion-induced transient currents generated by single ion hits were measured from the top electrode of sample by the 20 GHz oscilloscope (Tektronix, DPO 72004) via a linear amplifier (Picosecond Pulse Labs, 5840B) and a bias tee. The transient currents and their positional information were measured, and the two dimensional (2D) mapping of the transient currents was recorded. The spot size of the microbeam was about 1 μm in diameter. The microbeam was scanned from left to right and from bottom to top, and the scan area was 50×50 μm^2. A bias voltage ranging from -50 V to +50 V was applied to the top electrode of sample (the same side as ion incidence) and the bottom electrode was grounded. The variation of transient currents due to applied bias voltages was also investigated.

Energy depositions and creation of number of electron-hole pairs by incident ions were calculated by SRIM [14]. The calculation results are shown in Fig. 2. The projected ranges of 26 MeV-O and 45 MeV-Si in diamond were calculated to be 7.7 μm and 8.7 μm,

respectively. Therefore, 45 MeV-Si ions completely pass through the 6 μm-thick diamond membrane and 38.9 MeV (86.4%) of the energy was estimated to be deposited by electronic excitation. The diamond density of 3.515 g/cm^3 and the average ionization (electron-hole pair creation) energy of 13.2 eV [15] were used in these calculations.

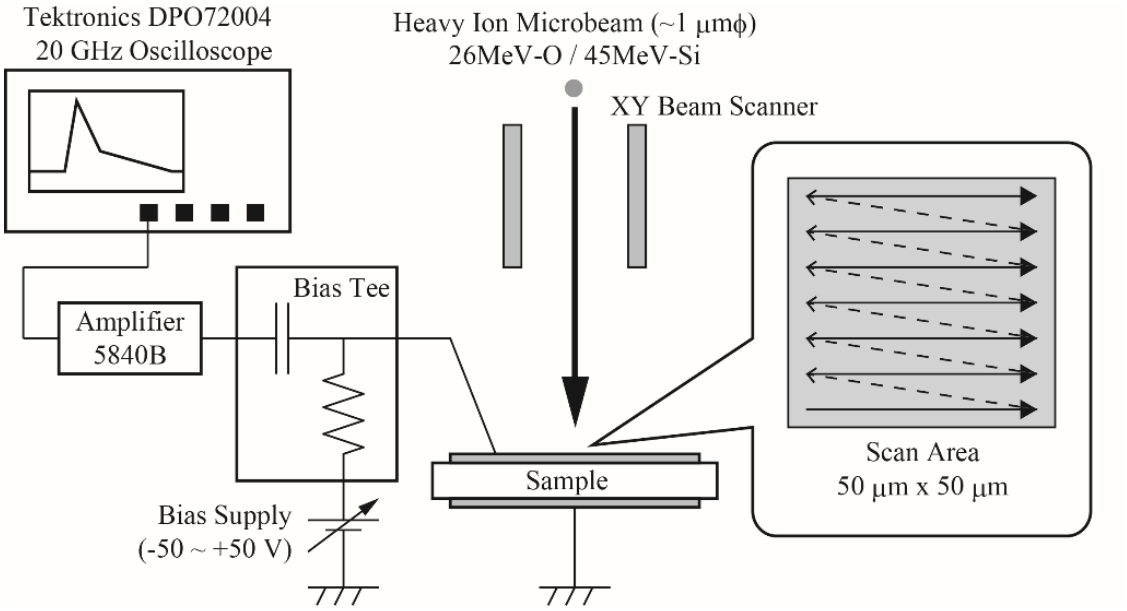

Fig. 1. Experimental setup of TRIBIC measurement.

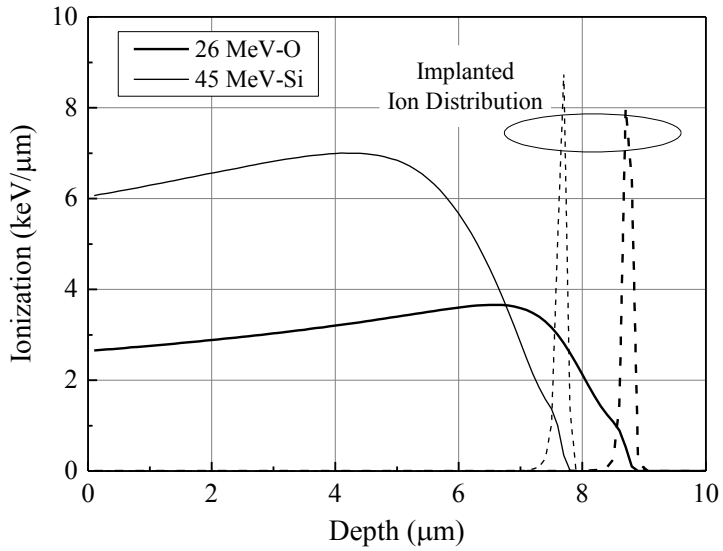

Fig. 2. Implanted ion distributions and deposited energy profiles of 26 MeV Oxygen and 45 MeV Silicon into diamond.

3. Results and Discussion

3.1. TRIBIC signals of 50 μm-thick diamond

Figure 3 shows the IV characteristics of the 50 μm-thick diamond. Although the IV characteristics indicates that the Ohmic contacts were incompletely formed, the capacitance was 5.35 pF independent of the bias voltage. Therefore, a uniform external electric field by the bias supply was formed throughout the diamond between the top and bottom electrodes.

Figure 4 shows typical transient currents (TRIBIC signals) at the biases of ±50 V (±10 kV/cm) when a single 26 MeV-O ion hit to the 50 μm-thick diamond. The linear amplifier was not used for this measurement. The signals at the positive bias were larger than the signals at the negative bias and no significant difference was observed in the width of signal. Collected charge was obtained by integrating transient current with respect to time and charge collection efficiency (CCE) was also obtained from the collected charge, the deposited ion energy, and the average ionization energy. The charge generated in 50 μm-thick diamond by 26 MeV Oxygen was estimated to be 0.318 pC. Figure 5 shows variations of the peak heights and CCEs of TRIBIC signals as a function of applied electric field. Both the peak height and the CCE increased with increasing absolute value of electric field. The value of CCE was higher at positive bias than at negative bias;

86.2 % at +10 kV/cm and 60.4 % at -10 kV/cm. This trend corresponds to the results reported elsewhere [4, 10]. According to the Shockley-Ramo theorem [16], in the case of charge generation near one electrode, CCE as a function of applied electric field can be explained by a single-carrier Hecht equation:

$$\mathrm{CCE} = \frac{(\mu\tau)E}{W}\left\{1 - \exp\left(-\frac{W}{(\mu\tau)E}\right)\right\} \quad (1).$$

Where W, E, and μτ are the thickness, the electric field, and the mobility-lifetime product, respectively. A uniform electric field in the diamond is assumed in Eq. (1). The fitting result is shown as the red line in Fig. 5. The values of μτ product were $(1.8\pm0.2)\times10^{-6}$ cm^2/V for holes and $(6.4\pm0.8)\times10^{-7}$ cm^2/V for electrons. These values are substantially lower than the values reported elsewhere [4, 10, 17, 18] which can be explained as follows. Firstly, since density of electron-hole pairs generated by swift heavy ions is much higher than that of light ions like protons and alpha particles, some carriers recombine promptly after generation, the value of CCE for swift heavy ions are generally lower than that for light ions [19]. As a result, the lower value of μτ product was obtained from the CCE for heavy ions than the reported values. Also, since we performed irradiation experiments using this sample prior to this study, significant radiation degradation might have been already caused even though diamond is super radiation tolerant.

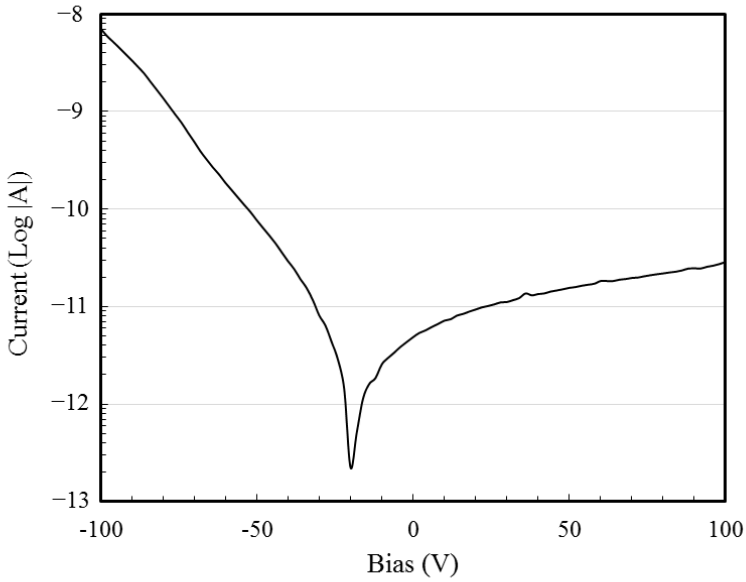

Fig. 3. Current-voltage characteristics of the 50 μm-thick diamond. Negative values in current were converted to the positive values in order to show in the semi-logarithmic scale.

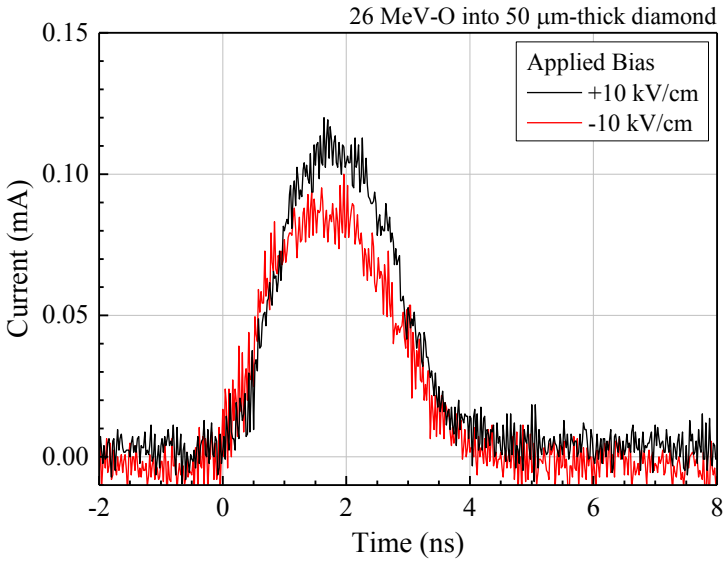

Fig. 4. Typical TRIBIC signals of the 50 μm-thick diamond generated by a single 26 MeV O^{5+} ion hit. The applied electric fields were +10 kV/cm (black) and -10 kV/cm (red). The linear amplifier was not used for this measurement.

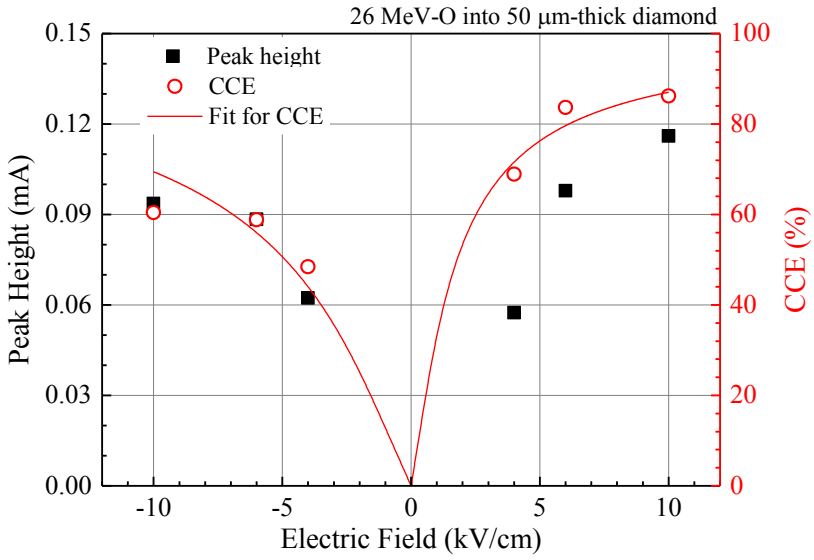

Fig. 5. Variations of peak height of TRIBIC signal (closed squares) and charge collection efficiency (CCE, red open circuits) of the 50 μm-thick diamond due to 26 MeV O^{5+} ion hits as a function of electric field. The line in red are the fitting curve of CCE by Eq. (1).

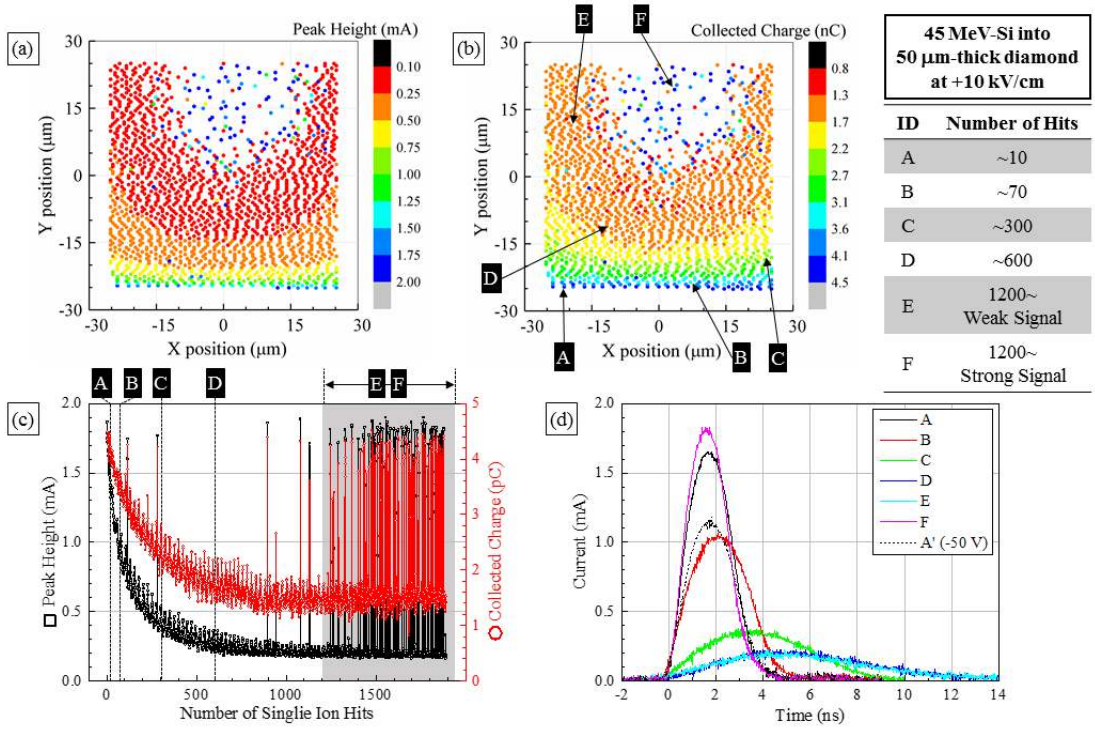

Fig. 6. (a) Two dimensional maps of peak height of TRIBIC signals and (b) collected charge induced by 45 MeV Si^{7+} ion hits. The applied bias was +50 V (+10 kV/cm) and the irradiation area was 50×50

μm^2. (c) Variations of the peak height (black) and the collected charge (red) as a function of number of single ion hits. (d) TRIBIC signals at the positions of A to F shown in (b). The number of hits at A to F are listed in the right table. A typical TRIBIC signal at the bias of -50 V (-10 kV/cm) is also shown in (d).

The TRIBIC measurement results of the 50 μm-thick diamond by 45 MeV Si^{7+} ion hits at +10 kV/cm are summarized in Fig. 6. Since the linear amplifier was used, the signal heights were much larger than the signals by 26 MeV O^{5+} ions in Fig. 4. Figs. 6(a) and (b) show the 2D maps of signal heights and collected charges of TRIBIC signals, respectively. Fig. 6(c) shows the variation of peak heights and collected charge as function of number of single ion hits. Fig. 6(d) shows typical TRIBIC signals at different XY positions and also the typical TRIBIC signal at -10 kV/cm (dashed line in black). These signals are identified by the letters of A to F and A', and their XY positions and the number of hits are shown in Figs. 6(b) and (c), respectively. These data were obtained by taking the average of ten TRIBIC signals around the number of hits shown in the table in the upper right of Fig. 6.

It was found from Fig. 6(c) that both the signal height and the collected charge decreased gradually with increasing number of hits. The increase in the width of the transient current in addition to the decrease in peak height appeared (see the signals A, B, C, and D in (d)). The microbeam was scanned from left to right, and from bottom to top, and the transient current was recorded only when the signal height was higher than a trigger level of the oscilloscope. Therefore, the signal amplitude was reduced gradually from the bottom left to the top right in the 2D maps and eventually the signal height fell below the trigger level. As a result, no signal was observed even if the ions hit, and the blank region appeared at

the upper region of 2D maps. Since a saturation tendency of decrease in TRIBIC signal which was observed after ~1000 hits was just due to the trigger level, the actual signal amplitude would continue to decrease after ~1000 hits. However, interestingly, strong signals appeared sparsely at the upper region of 2D mapping (after ~1200 hits, see the shaded zone in (c)). The typical weak and strong TRIBIC signals were shown as the signals E and F in (d). The shape of signals E and F was unchanged from signals D and A, respectively.

These results are obviously attributable to the polarization effect. When ion induced carriers (electrons and holes) are trapped in deep levels in diamond, the trapped carriers interfere with the external electric field and the charge collection is interrupted. The detail of polarization effect is discussed in section 3.3. We therefore conclude that the inhomogeneous 2D maps in Figs. 6(a) and (b) do not indicate the inhomogeneity of crystal quality, but are simply caused by enhancing the polarization effect with increasing number of ion hits. The results of Fig. 6 also indicate that the polarization effect induced by previous ion hits are widely spread bidimensionally and the degradation of signal amplitude occurs even if the position of subsequent ion hits is different from that of precedent ion hits. The spatial distribution of the polarization effect could be estimated to be over the range of microns, although it is difficult to estimate the exact value in this study.

The strong signal F occasionally observed after 1200 hits were comparable to the signal before the polarization occurred (the signal A), and the weak signals (the signal E) appeared for a while after a strong signal appeared once. It is speculated that the

polarization effect was temporarily cleared out by excess accumulation of carriers due to the repetition of ion hits [9]. On the other hand, the polarization effect is polarity-dependent and the inhomogeneous mapping was never observed when the negative bias was applied. Also, the signal height at -10 kV/cm, which is shown as the signal A' in Fig. 6(d), was about 60% compared to the signal at +10 kV/cm.

3.2. TRIBIC signals of 6μm-thick diamond membrane

The TRIBIC signals of the 6 μm-thick diamond membrane by 45 MeV Si^{7+} ion hits are summarized in Fig. 7. Figures 7(a) and (b) show the 2D maps of peak height of TRIBIC signals at the biases of -3 V (-5 kV/cm) and +3 V (+5 kV/cm), respectively. The 2D maps of collected charges are not shown here since they were qualitatively no different from that of peak heights. The ion irradiation at a strong positive bias (+50 kV/cm) was performed just before the TRIBIC measurements and "island" structure appeared in the 2D map. Examples of TRIBIC signals at ±5 kV/cm are shown in (c) and (d), respectively. These signals are identified by the letters of G to K and their locations are listed in the table in Fig. 7. Figures 7(d) and (e) show the histograms of peak height and collected charge, respectively.

At the negative bias condition (Fig. 7(c)), the signals at the islands (the signal G) were stronger than the signals at the other region (the signal H). Meanwhile, at the positive bias condition (Fig. 7(d)), the signals at the other region (the signal K) were stronger than that at the islands (the signal I). In addition, the weaker signals were found at the coast of islands (the signal J). The signals at the other region appeared sparsely, indicating most of signals generated by ion hits at the other region were below the trigger level (~0.2 mA)

and could not be detected by the oscilloscope. The signal height at the other region at -5 kV/cm (the signal H) was about 60% compared to +5 kV/cm (the signal K).

The trend observed at the other region is very similar to the result of Fig. 6, indicating the polarization effect could also appear in the 6 μm-thick diamond membrane. Although the polarization effect has been often observed in diamond whose thickness is considerably longer than projected range of ions, swift heavy ions which have high electronic energy deposition can induce the polarization effect even if diamond is thin enough for ions to penetrate. On the other hand, the signals at the islands showed a different trend from the other region, suggesting the existence of dislocation, inclusion, or grain boundary. The difference of bias polarity dependence is thought to be due to the difference of crystal quality in the islands. It is unclear at the present stage whether the island structure was formed during crystal growth or during the RIE etching for the fabrication of membrane structure.

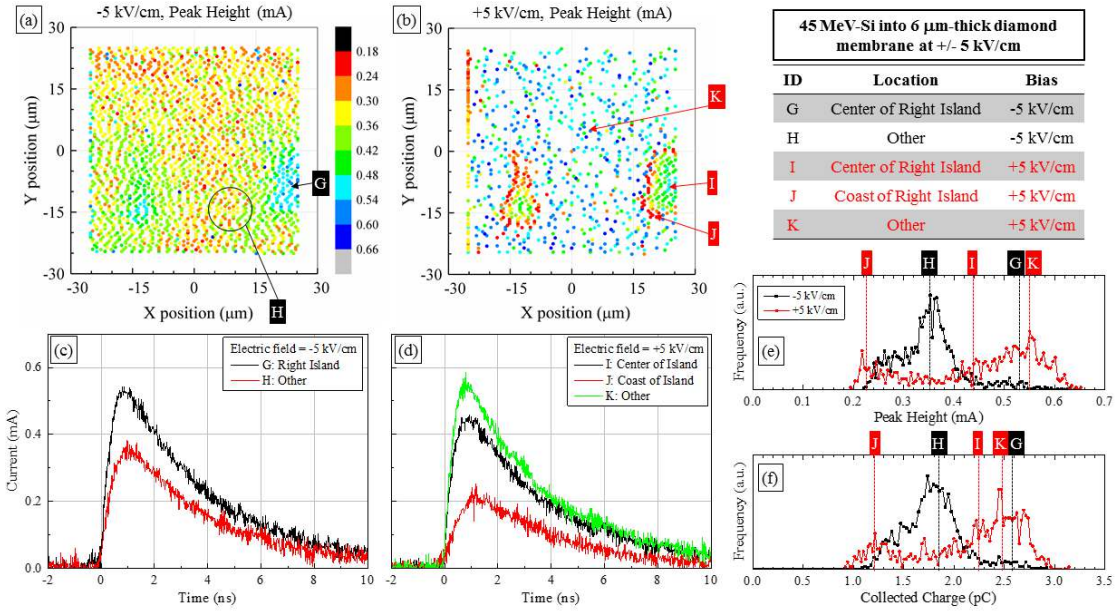

Fig. 7. Summary of TRIBIC data in the 6 μm-thick diamond membrane due to 45 MeV Si^{7+} ion hits at ±5 kV/cm. (a) and (b) show the 2D maps of the peak heights at -5 kV/cm and +5 kV/cm, (c) and (d) show typical transient currents at -5 kV/cm and +5 kV/cm, respectively. (e) and (f) are histograms of the peak height and the collected charge, respectively.

3.3. Analysis of the polarization effect based on the Shockley-Ramo theorem

In order to analyze the signal degradation due to the polarization effect shown in Fig. 6(d), a simulation of transient currents based on the Shockley-Ramo theorem developed by Li et al. [20] was performed. A one-dimensional model of charge collection in semiconductors can be obtained from the Shockley-Ramo theorem and this is suitable to clarify how the polarization effect affects the charge collection process. Figure 8(a) shows the conceptual diagram of the model proposed in this study. It was assumed that an electric field was formed uniformly in diamond and the polarization occurred only in the irradiated region. In this case, the transient current, $i(t)$, is represented by the following equations:

$$i(t) = i_e(t) + i_h(t) \tag{2}$$

$$i_e(t) = \frac{q}{GW}\exp\left(-\frac{t}{\tau_e}\right)\int_0^W \Lambda(x,t)\cdot v_e(x)\,dx \tag{3}$$

$$i_h(t) = \frac{q}{GW}\left\{\int_0^R \Lambda(x,t)\cdot v_h(x)\cdot\exp\left(-\frac{t}{\tau_{h1}}\right)dx + \int_R^W \Lambda(x,t)\cdot v_h(x)\cdot\exp\left(-\frac{t}{\tau_{h2}}\right)dx\right\} \tag{4}.$$

Where $i_e(t)$, $i_h(t)$, and t denote the electron current, the hole current, and the time, respectively. q, Λ, G, R, and W are the electron charge, the electronic energy deposition by incident ions, the average ionization energy (13.2 eV [15]), projected range of incident ions, and the sample thickness. The data of $\Lambda(x,\ t = 0)$ was obtained from Fig. 2. The electron lifetime, τ_e was assumed to be constant for the polarization effect. On the other

hand, it was assumed that the hole lifetime in the irradiated region ($0 \leq x \leq R$), τ_{h1} was reduced by the polarization effect and the hole lifetime in the other region ($R< x \leq W$), τ_{h2} was unchanged. The drift velocity, v is represented by the Canali model [21]:

$$v_i = \frac{\mu_i E(x)}{1+\frac{\mu_i E(x)}{v_{si}}} \qquad i = e, h \qquad (5).$$

Where μ, v_s, and E are the drift mobility, the saturation velocity, and the electric field. The subscripts, e and h denote electron and hole, respectively Constant values were used for both the electron and the hole mobilities, and the drift velocity was changed only by the change in electric field. Values of 1.5×10^7 cm/s and 1.05×10^7 cm/s were used for electron and hole saturation velocity [2]. Finally, the calculated current was convolved with a Gaussian that included all terms of the system resolution, such as stray capacitance, etc. The typical response time was 6.5×10^{-10} s for the 50 μm-thick diamond and 3.0×10^{-10} s for the 6 μm-thick diamond membrane.

Initial values of mobility and lifetime were determined from fittings of the signals A and A' in Fig. 6(d), which were the transient currents without polarization. The obtained values are summarized in Table 1 and the fitting results are shown in Fig. 8(b). The products of mobility and lifetime for electrons and holes in Table 1 were slightly smaller than the μτ products which were obtained in Fig. 5. This is attributed to the difference of incident ions [19].

Table 1. Parameters used for the simulation of transient currents in Fig. 6(d).

Electron mobility, μ_e (cm^2/Vs)	2.2×10^2
Hole mobility, μ_h (cm^2/Vs)	3.1×10^2

Electron lifetime, τ_e (ns)	2.4
Hole lifetime, τ_{h1} (ns)	5.45
Hole lifetime after polarization, τ_{h2} (ns)	1.1
Electric field after polarization, E_p (V/cm)	5.0×10^2

Although the polarization effect simply induces the reduction of electric field in diamond according to the general understanding, it was shown from the simulation study that the decrease in hole lifetime should also be taken into account to fit degraded transient currents after the polarization. Assuming both the electric field and the hole lifetime are reduced by the polarization effect only in the irradiated region ($0 \leq x \leq R$), transient currents were calculated and the results for the 50-μm thick diamond are illustrated in Fig. 8(b). In Fig. 8(b), the experimental transient currents as well as the calculated results are shown. The signal D, which is the transient current after the polarization, could be simulated by considering both the decrease in hole lifetime and electric field in the irradiated region. The results showed the hole lifetime and the electric field were reduced from 5.45 ns and +10 kV/cm and to 1.1 ns and +0.50 kV/cm, respectively.

This model also explains well the transient currents in the 6-μm thick diamond membrane. 45 MeV-Si ions completely penetrate the 6-μm diamond membrane and induce the polarization, i.e. the decrease in both electric field and hole lifetime, throughout the depth direction. In this case, however, the electron current is comparable with the hole current and we were unable to determine individual parameters for electrons and holes. Therefore the same parameters were used for electrons and holes to simulate the signal K. The results are shown as blue lines in Fig. 8(c). The calculated transient current was in

agreement with the signal J when the electric field and hole lifetime were reduced from +5.0 kV/cm and 5.0 ns to +2.0 kV/cm and 3.0 ns, respectively. Further discussion should be conducted for the change in electron lifetime in the irradiated region, although no variation of electron lifetime was assumed in this study. Since the polarization effect is observed at the condition of positive bias only, it is difficult to discuss the existence of electron lifetime killer at the present stage.

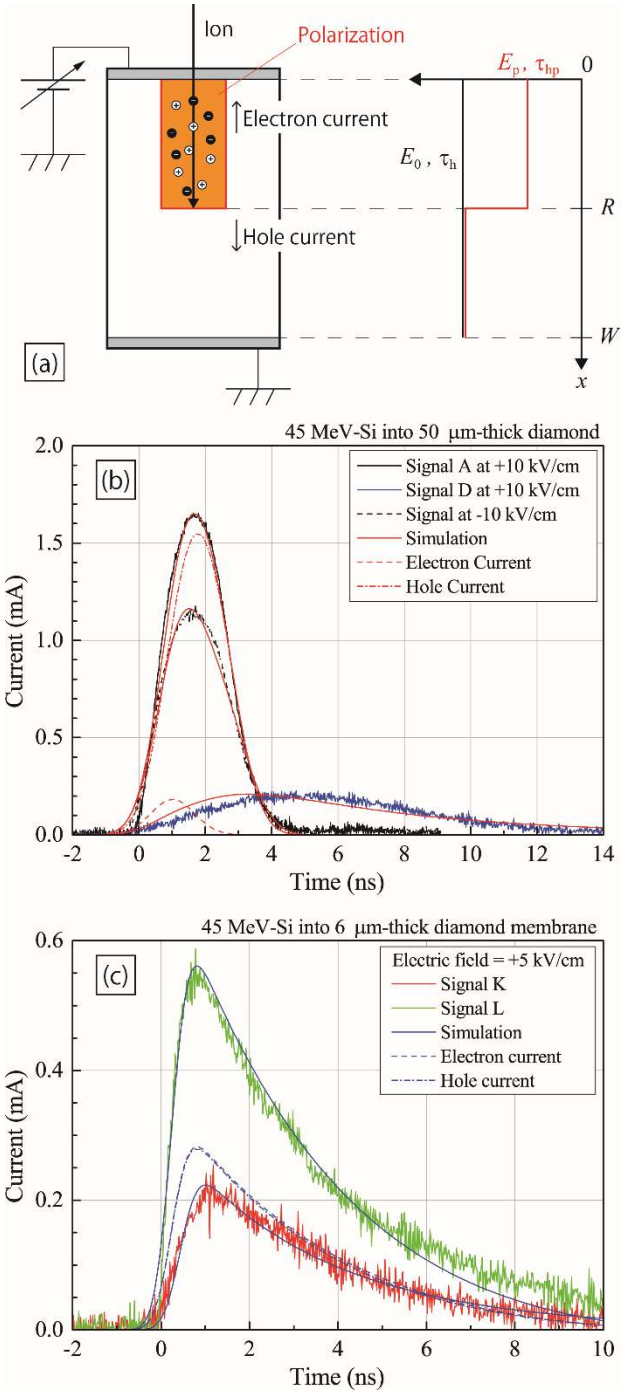

Fig. 8. (a) One-dimensional model of the polarization effect based on the Shockley-Ramo theorem. (b) and (c) are calculation results of the 50 μm-thick diamond (red lines) and the 6 μm-thick diamond membrane (blue lines), respectively. Electron and hole currents are drawn as the dashed and dashed-dotted lines, respectively.

4. Conclusion

Transient currents (TRIBIC signals) of diamonds induced by single swift heavy ion hits and their 2D mappings were investigated in this study. Variations of TRIBIC signals and CCEs due to different diamond thicknesses, applied biases, and bias polarities were clarified. Change in the TRIBIC signals by subsequent of ion hits was also investigated.

From the results of TRIBIC measurements in the 50 μm-thick diamond by irradiated by 45 MeV-Si ions, the signal degradation and instability originating from the polarization effect were observed. At positive bias, signals were drastically degraded by the subsequent ion hits and became unstable with increasing number of ion hits. An increase in the charge collection time in addition to the decrease in signal height were observed. After 1200 ion hits, non-degraded signals appeared occasionally with fully degraded signals. The spatial distribution of the polarization effect could be estimated to be in the range of microns. At negative bias, on the other hand, neither signal degradation nor instability of TRIBIC signals appeared with the subsequent of ion hits. The signal height at negative bias was about 60% compared to the signal height at positive bias.

The similar trend was found in the TRIBIC results of the 6 μm-thick diamond membrane by 45 MeV-Si ion hits. This fact strongly indicates that the polarization effect could occur in diamond membranes by swift heavy ions. Island structure was found in the 2D maps and signals in the islands showed different trend from the other regions. The inhomogeneity is thought to be caused by the presence of dislocation, inclusion or grain boundary in diamond.

Also, simulation study based on the Shockley-Ramo theorem was performed to understand the observed polarization effect. The proposed model explains well transient currents in both thick and thin diamond. It was shown from the simulation study that the polarization occurred only in the irradiated region and induced significant reduction of hole lifetime in addition to electric field.

Acknowledgement

This work was supported by JSPS KAKENHI Grant Number 26249149. Sandia National Laboratories is a multi-program laboratory managed and operated by Sandia Corporation, a wholly owned subsidiary of Lockheed Martin Corporation, for the U.S. Department of Energy's National Nuclear Security Administration under contract DE-AC04-94AL85000.

References

[1] S. F. Kozlov, E. Belcarz, M. Hage-Ali, R. Stuck, and P. Siffert, Nucl. Instr. Meth. 117 (1974) 277-283.

[2] F. Nava, C. Canali, M. Artuso, E. Gatti, P. F Manfredi, and S. F. Kozlov, IEEE Trans. Nucl. Sci. NS-26 (1979) 308-315.

[3] For example: V. Grilj, N. Skukan, M. Pomorski, W. Kada, N. Iwamoto, T. Kamiya, T. Ohshima, and M. Jakšić, Appl. Phys. Lett. 103 (2013) 243106-1-4.

[4] M. Tsubota, J. H. Kaneko, D. Miyazaki, T. Shimaoka, K. Ueno, T. Tadokoro, A. Chayahara, H. Watanabe, Y. Kato, S. Shikata, and H. Kuwabara, Nucl. Instr. Meth. A 789

(2015) 50-56.

[5] S. F. Kozlov, R. Stuck, M. Hage-Ali, and P. Siffert, IEEE Trans. Nucl. Sci. NS-22 (1975) 160-170.

[6] W. Kada, N. Iwamoto, T. Satoh, S. Onoda, V. Grilj, N. Skukan, M. Koka, T. Ohshima, M. Jakšić, and T. Kamiya, Nucl. Instr. Meth. B 331 (2014) 113-116.

[7] Y. Sato and H. Murakami, Jpn. J. Appl. Phys. 4 (2015) 096401-1-5.

[8] G. Gervino, S. Bizzaro, C. Palmisano, and L. Periale, Nucl. Instr. Meth. A 718 (2013) 325-326.

[9] Y. Sato, T. Shimaoka, J. H. Kaneko, H. Murakami, M. Isobe, M. Osakabe, M. Tsubota, K. Ochiai, A. Chayahara, H. Umezawa, and S. Shikata, Nucl. Instr. Meth. A 784 (2015) 147-150.

[10] V. Grilj, N. Skukan, M. Jakšić, W. Kada, and T. Kamiya, Nucl. Instr. Meth. B 306 (2013) 191-194.

[11] H. Schone, D. S. Walsh, F. W. Sexton, B. L. Doyle, P. E. Dodd, J. F. Aurand, R. S. Flores, and N. Wing, IEEE Trans. Nucl. Sci. 45 (1998) 2544-2549.

[12] M. Pomorski, B. Caylar, and P. Bergonzo, Appl. Phys. Lett. 103 (2013) 112106-1-4.

[13] M. B. H. Breese, E. Vittone, G. Vizkelethy, and P. J. Sellin, Nucl. Instr. Meth. B 264 (2007) 345-360.

[14] Available at: <http://www.srim.org>

[15] C. Canali, E. Gatti, S. F. Kozlov, P. F. Manfredi, C. Manfredotti, F. Nava, and A. Quirini, Nucl. Instr. Meth. 160 (1979) 73-77.

[16] E. Vittone, F. Fizzotti, A. Lo Giudice, C. Paolini, C. Manfredotti, Nuc. Instr. Meth. B 161 (2000) 446-451.

[17] A. Lohstroh, P. J. Sellin, S. G. Wang, A. W. Davies, J. Parkin, R. W. Martin, and P.

R. Edwards, Appl. Phys. Lett. 90 (2007) 102111-1-3.

[18] A. Galbiati, S. Lynn, K. Oliver, F. Schirru, T. Nowak, B. Marczewska, J. A. Dueñas, R. Berjillos, I. Martel, and L. Lavergne, IEE Trans. Nucl. Sci. 56 (2009) 1863-1874.

[19] T. Ohshima, N. Iwamoto, S. Onoda, G. Wagner, H. Itoh, and K. Kawano, Surf. Coat. Tech. 206 (2011) 864-868.

[20] Z. Li and H. W. Kraner, Nuclear Physics B (Proc. Suppl.) 32 (1993) 398-409.

[21] C. Canali, G. Majini, R. Minder, and G. Ottaviani, IEEE Trans. Electron Dev. 22 (1975) 1045-1047.